Chapter 1

Fiber Optic and Free Space Michelson Interferometer — Principle and Practice

Michal Lucki, Leos Bohac and Richard Zeleny

Additional information is available at the end of the chapter

http://dx.doi.org/10.5772/57149

1. Introduction

Michelson interferometer is used in metrology of small amplitude nonelectric physical quantities for its accuracy, noncontact and noninvasive procedure. It is broadly used in sensor applications. There are many papers assuming the use of an interferometer and focusing on measured results, but there are not many works offering practical knowledge on how to construct and run Michelson interferometer. In this chapter we discuss wide range of aspects, which greatly facilitate the launch of Michelson interferometer in in-situ conditions.

Random addition to a signal can practically disqualify many techniques for their eventual application in accurate measurements of displacement or vibrations. The interferometric method is suitable for signals that require a noninvasive and noncontact method [1]. It allows avoiding a physical contact with a measured object that would originate spurious signals causing errors greater than the values to be measured. Such signals may be encountered in industrial applications like mining or construction technologies, in measurements of resonant frequencies of machines or bridges and last but not least in the measurement of small deformations or spatial distributions of temperature. Finally, measurements performed in harsh environment, such as the ones with extremely high temperature, could damage the measuring apparatus. In addition, the interferometric method is attractive for its price.

2. Principle of the method

The necessary and sufficient condition to observe interference of light is the coherence length being greater than optical path difference between two superposed beams. In practice,

interference is considered for coherent waves, where the maximum distance from the light source, at which interference is observed, is related to the spatial cross-correlation between two points in a wave for an arbitrarily selected time instant.

A very good description of interference observed in Michelson interferometer as well as many practical aspects about running experiment with Michelson setup is presented in [2]. A numerical model of a Michelson interferometer is published in [3]. A block scheme of a Michelson interferometer is presented in Figure 1. Based on the scheme, in the following section, we present the mathematical model of light interference in a free space Michelson interferometer.

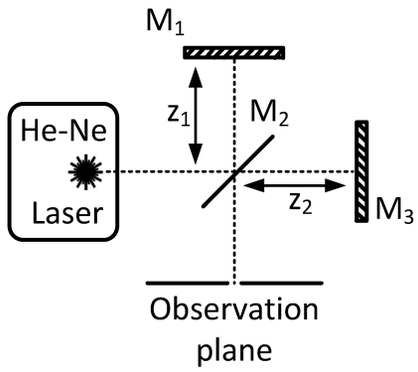

Figure 1. Schematic diagram of a Michelson interferometer. M_2 – 50% mirror (beam splitter), M_1, M_3 – dielectric mirrors.

2.1. Interference of light observed in a free space Michelson interferometer

Let us consider a wave entering the Michelson interferometer, presented in Figure 1.

$$E = E_0 \sin\left(kz - \omega t + \varphi_0\right) \tag{1}$$

Where k is known as angular wavenumber that is to express the magnitude of the wave vector, and for dielectrics is as:

$$k = \frac{2\pi}{\lambda} \tag{2}$$

And ω is angular frequency. Knowing the frequency of light ν having a wavelength λ and a speed c, it can be written as:

$$\omega = 2\pi\nu = 2\pi\frac{2}{\nu} \tag{3}$$

http://dx.doi.org/10.5772/57149

For simplicity and without restricting generality, we assume certain time instant where φ_0 is equal to 0.

$$E = E_0 \sin(kz - \omega t) \tag{4}$$

The wave is split at a beam splitter in Michelson interferometer and two waves E_1 and E_2 are formed. The wave that is partially reflected at the beam splitter M_2 and is reflected at M_1 mirror can be written as:

$$E_1 = E_{01} \sin(kz_1 - \omega t) \tag{5}$$

The wave transmitted through the beam splitter and reflected from M_3 mirror is as:

$$E_2 = E_{02} \sin(kz_2 - \omega t) \tag{6}$$

where z_1 is optical path length from the beam splitter (M_2) to M_1 mirror, z_2 is optical path length from the beam splitter (M_2) to M_3 mirror, as displayed in Figure 1.

E_0 amplitude is split to E_{01} and E_{02}. In theory, both waves do not have any phase shift with regard to each other as well as in an ideal case the splitter should separate them symmetrically. In real Michelson setup, splitting is not symmetrical and the amplitudes of split waves are:

$$E_{01} = E_0 \cdot r_2 \cdot r_1 \tag{7}$$

$$E_{02} = E_0 \cdot t_2 \cdot r_3 \tag{8}$$

Where r_2 is the reflection coefficient of a beam splitter, r_1 is the reflection coefficient of M_1 mirror, t_2 is the transmission coefficient of a beam splitter, and r_3 is the reflection coefficient of M_3 mirror. In addition, in practical consideration, the phase of E_2 wave transmitted through the beam splitter is changed, as referred to the phase of E_1. Then, they should be denoted as:

$$E_1 = E_{01} \sin(kz_1 - \omega t) \tag{9}$$

$$E_2 = E_{02} \sin(kz_2 - \omega t + \varphi) \tag{10}$$

The superposition of interfering waves at the beam splitter is the sum of both waves, denoted as E_3:

$$E_3 = E_1 + E_2 = E_{01}\sin(kz_1 + \omega t) + E_{02}\sin(kz_2 + \omega t + \varphi) \tag{11}$$

A photodetector detects light intensity I related to intensity of electric field E, as in (12):

$$I \sim E^2 \tag{12}$$

For I_3 as the intensity related to E_3 it can be written:

$$I_3 \sim \left[E_{01}\sin(kz_1 + \omega t) + E_{02}\sin(kz_2 + \omega t + \varphi)\right]^2 \tag{13}$$

$$\begin{aligned} I_3 \sim & E_{01}^2 \sin^2(kz_1 + \omega t) + 2E_{01}E_{02}\sin(kz_1 + \omega t)\sin(kz_2 + \omega t + \varphi) + \\ & + E_{02}^2 \sin^2(kz_2 + \omega t + \varphi) \end{aligned} \tag{14}$$

To simplify, the following trigonometric operation can be performed on second term:

$$2\sin\alpha \cdot \sin\beta = \cos(\alpha - \beta) + \cos(\alpha + \beta) \tag{15}$$

We obtain:

$$\begin{aligned} I_3 \sim & E_{01}^2 \sin^2(kz_1 + \omega t) + E_{01}E_{02}\cos\left[k(z_1 - z_2) - \varphi\right] + \\ & + E_{01}E_{02}\cos\left[k(z_1 + z_2) + 2\omega t + \varphi\right] + E_{02}^2 \sin^2(kz_2 + \omega t + \varphi) \end{aligned} \tag{16}$$

It can be noticed that second term $E_{01}E_{02}\cos\left[k(z_1 - z_2) - \varphi\right]$ is time independent, first and fourth terms oscillate at ω, third term oscillates at 2ω. Using this value of λ and the speed of light being c=3x10^8 m.s^{-1}, the frequency of light ν is calculated as in (3). Since the *sin* term of the first and last term oscillates at this frequency, the *cos* term oscillates at double of this frequency, the frequency changes are too fast for a detector to react (it is few ranges slower) [2]. It instead measures average value of these terms. For sin^2 term it is 0.5 and for *cos* it is 0. Eq. (16) can be rewritten to:

$$I \sim \frac{1}{2}E_{01}^2 + \frac{1}{2}E_{02}^2 + E_{01}E_{02}\cos(k\Delta z - \varphi) \tag{17}$$

where Δz is optical path difference:

$$\Delta z = z_1 - z_2 \tag{18}$$

http://dx.doi.org/10.5772/57149

Intensity I is maximum if and only if *cos* term is equal to 1, i.e. when $k\Delta z$-φ is zero or multiple of 2π. Minimum intensity is if and only if *cos* term is equal to -1. Then, it can be written:

$$I_{\max} \sim \frac{1}{2}E_{01}^2 + \frac{1}{2}E_{02}^2 + E_{01}E_{02} = \frac{1}{2}\left(E_{01} + E_{02}\right)^2 \tag{19}$$

$$I_{\min} \sim \frac{1}{2}E_{01}^2 + \frac{1}{2}E_{02}^2 - E_{01}E_{02} = \frac{1}{2}\left(E_{01} - E_{02}\right)^2 \tag{20}$$

Light intensity depends on the optical path difference Δz. If the optical path difference of both interferometer's arms is equal or is multiple of 2π, there is constructive interference and the intensity of interference fringes is maximum.

The above model refers to a free space Michelson interferometer. The mathematical apparatus for a fiber optic Michelson interferometer can be more extensive, since one could consider the reflections at connectors, fiber dispersion, as well as the properties of polarizers, a coupler and the optional presence of a fiber stretcher. However, the model reflects the general idea on light interference in any Michelson interferometer.

3. Experimental setup

When planning how to arrange an experiment using an interferometer, the choice can be made between large number of interferometers, as for example Michelson interferometer [4], Mach-Zehnder interferometer [5], Sagnac interferometer [6], Fabry Perot interferometer, and last but not least Fizeau interferometer, Twyman-Green interferometer, Nomarski interferometer [7]. The selection of interferometer is not always arbitrary; it must be suited to the application. In addition, it is possible to build up an interferometer with a free space or a fiber optic arrangement. The Michelson and Mach-Zehnder are the most widely used interferometers. Michelson interferometer is used for its simplicity, accuracy, and lower number of components. In this paper we focus on the Michelson interferometer, in which both interference beams propagate in their arms twice on the contrary to Mach-Zehnder interferometer, which is simpler and easier to implement. The Michelson interferometer also provides easier calibration and better control of mechanical stability.

Obtaining interference fringes is just one of many steps in the measurement procedure. Another step is the integration of a measured object with the interferometer. Transparent objects can be inserted into a beam path in one arm. Other objects should be placed at the end of the interferometer arm or fixed to the mirror.

There is a number of aspects fundamental for experiment like thermal stability of light source used, as well as its coherence length. The experimental setup must suppress ambient vibrations responsible for the spurious signal and thus it must be mechanically stable; otherwise the

interference pattern is not stable in time. Especially in free space arrangement, where mechanical stability of the setup is required, the use of optical table suppressing vibrations is practically unavoidable. Fiber optic arrangement can suppress disturbing signals, since signal is guided in optical fibers, whose length is barely influenced by mechanical instability.

An interferometer should be mounted on a pneumatic laboratory table, for example in the faculty cellars where vibrations of ground are minimal, and mounted by using special holders. In very accurate measurements, where measured quantity is a multiple of the wavelength, it is necessary to use lasers with good temperature stability of a wavelength.

3.1. Free space Michelson interferometer

In free space Michelson interferometer, it is suitable to use a laser from the visible range to facilitate calibration and data reading, for example a He-Ne laser, which exhibits good wavelength stability (approximately 2 MHz). In free space Michelson interferometer, the position of mirrors and a beam splitter is adjusted by observing the incident light in the interference plane. Although this arrangement is very sensitive to mechanical instability, the fringes can be obtained employing a systematic approach. To calibrate the interferometer, the angles between mirrors are adjusted as well as proper angles between the beam splitter and mirrors are set to get the interference pattern with required number of fringes.

Adjusting the position of a beam splitter affects both beams at once and is more time consuming. The position of both dielectric mirrors should be set, and once both beams overlap at the beam splitter, the position of all elements of the setup is adjusted to set right distribution of fringes in the observation plane. The increase in arm's length by the distance equal to the value of the half of the wavelength (316.4 nm) causes the change to the phase difference between two beams equal to 2π (one interference fringe). The interferometer is then able to measure displacement in a range of several hundred nanometers (corresponding to the ability to distinguish one fringe) [8].

The concept of a free space Michelson interferometer with a sample investigated object and a connected detector is displayed in Figure 2. A He-Ne laser is one of very broadly used in free space implementations because it emits light from the visible range and exhibits great wavelength stability and decent output power. A laser beam is split into two beams by a beam splitter (M_2), (amplitude splitting does not affect polarization). Each beam is propagated along its optical path controlled by a mirror system (M_1, M_3). The reference beam is guided to the observation plane going twice through the beam splitter. The measuring beam is guided to the investigated object, a copper rod terminated with a dielectric reflecting mirror. (It can potentially be any other object specific for its length, and being solid in the investigated range of temperatures). Measured signal affects the position of the M_3 mirror placed at its end and causes changes to the reflected optical path length in a measuring arm.

The reference and measuring beams interfere at the beam splitter. An additional phase shift between both arms causes changes to the distribution of interference fringes that are counted and monitored. Information about the amount of fringes is stored in a computer and is used to calculate the change in optical path length. Number of fringes passing through the aperture

http://dx.doi.org/10.5772/57149

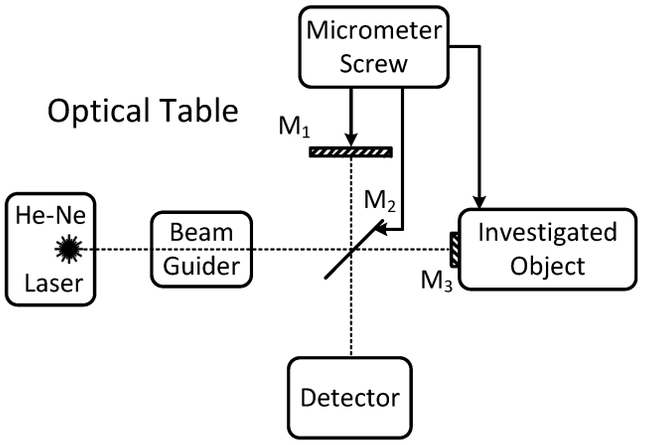

Figure 2. Schematic diagram of a free-space Michelson interferometer. M_2 – 50% mirror (beam splitter), M_1, M_3 – dielectric mirrors.

in an observation plane is proportional to the measured quantity. Sample interferograms obtained in an exemplary experiment are shown in Figure 3.

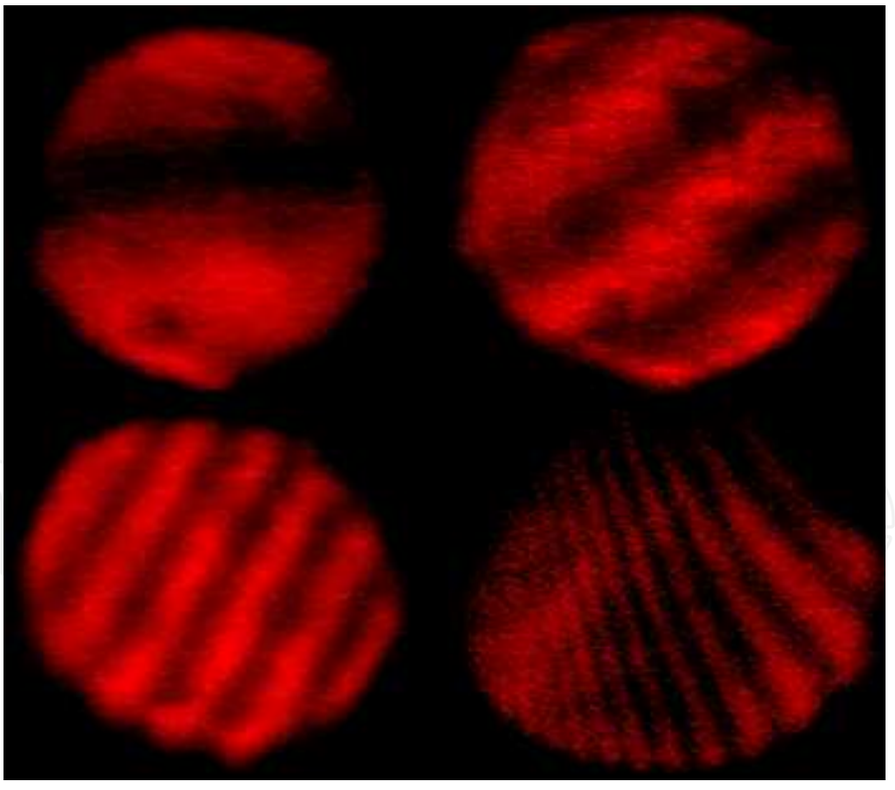

Figure 3. Sample distribution of interference fringes. Mirrors adjusted to one dark fringe (top left), two light and two dark fringes (top right), new fringes appearing when taking measurement (bottom left), changed fringe direction caused by different angle between M_1 and M_3 mirrors (bottom right).

Figure 4. Sample time variation of light intensity at the output of an interferometer measured and displayed on an oscilloscope. Two marked maximum points show one fringe period corresponding to the phase shift of 2π, which means the arm length is changed by the length of the propagated wave.

Considering the fact that fringes pass through the surface of a photodetector, a signal detected by a photodiode or eventually displayed on an oscilloscope contains many minima and maxima of light intensity, such as one displayed in Figure 4. This may be the signal you see after launching the measurement, indicating that the setup started to work. If the interferogram is stable in time and the detected light intensity is a constant value, it means that the investigated object generates no signal or there is no interference for any reason (for example there is a problem with the coherence length of used light source or a detector detects light from one arm only), which in practice can be very confusing. The use of visible light facilitates to verify the existence of interference fringes. In free space interferometers, performing the measurement in the visible spectrum is appropriate because of exact calibration based on a visual control. In fiber optic interferometer, the use of visible light is rather impossible because most of optical fibers are transparent for longer wavelengths.

3.2. Fiber optic Michelson interferometer

Fiber optic Michelson interferometer employs the same principle of splitting a laser beam and inserting the optical path difference between the arms. Both waves interfere at a coupler. However, there are many features specific for fiber optic interferometers, disregarding the fact that we deal with the Michelson interferometer. Essential modifications result from the fact that light is guided in optical fibers. The concept of a fiber optic Michelson interferometer with connected detector is displayed in Figure 5.

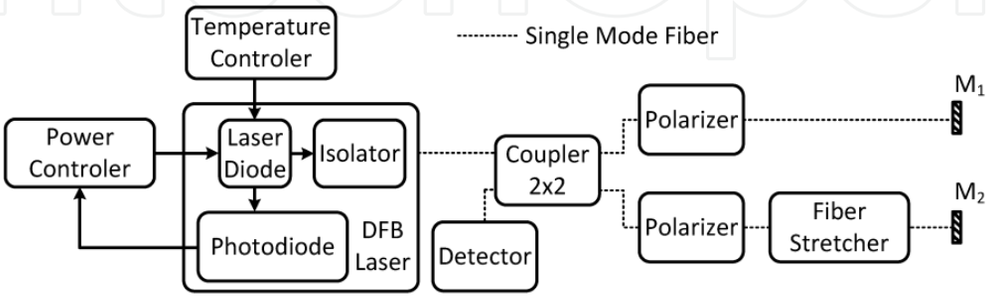

Figure 5. Schematic diagram of a fiber-optic Michelson interferometer. M_1, M_2 – dielectric mirrors.

http://dx.doi.org/10.5772/57149

Fiber mirrors and a coupler should be compatible with the used laser. In theory, they are designed to work at a specific wavelength, but in practice, cheap fiber mirrors are created by using dielectric material and they are broadband. Pigtailed fiber mirrors are commercially available. For example, if you have a mirror labeled as operating at 1310 nm, it is likely that it exhibits high reflectance also at 1550 nm. However, in case of fiber couplers, the splitting ratio, important for fringe thickness and contrast, can be very different at both wavelengths.

Calibration of a fiber optic interferometer requires using additional components, compared to a free space interferometer, where optical path length can be simply adjusted by positioning of mirrors. In fiber optic Michelson interferometer the path length can be increased by inserting an air gap between two fibers, which results in additional losses at the aperture and abandoning the ideal of all-fiber interferometer. One of the most spread techniques is to use a fiber stretcher. A silica fiber is elastic and can be mechanically stretched by about 2 % [9]. It allows for changing the optical path length necessary for the exactly out of phase beams and the near-zero light intensity at a detector. The silica fiber can be stretched by using a cylinder made of a rubber material placed between retainers, which are precisely tightened to each other by using a micrometer screw. Consequently, the cylinder expands and the fiber is stretched, however with the sub-millimeter precision insufficient for the phase adjustment of the light wave. Thus, for a sub-micrometer stretch, a piezoelectric actuator [10] with the voltage control is optimal. Electric field applied to the actuator below its Curie point causes the ions shifts, (an elastic strain), resulting in linear increase (or decrease) in length of the actuator according to the electric field polarity. This feature refers to crystals with no center of symmetry, such as quartz, lithium niobate or bismuth titanate. Most of commercially available fiber stretchers provide the optical path length variation of few micrometers per volt. The fiber stretch is frequency dependent, which should be taken into account, when alternating current is applied to an actuator.

Polarizers in a fiber optic Michelson interferometer are necessary to avoid random polarization due to stretches or birefringence resulting in intensity instability. It can improve the stabilization of visibility in fiber optic sensors [11]. Instead of polarizers that are source of insertion losses, it is suitable to use polarization maintaining fibers.

3.3. Lasers for interferometers

The fiber optic Michelson interferometer require the use of lasers operating at telecommunication wavelengths since optical fibers transmit optical radiation in the range of about 800 – 1600 nm. Helium-Neonium laser, very popular in free space optics, cannot be used with most of commercially available fibers. Distributed Feedback Lasers (DFB) operating at any wavelength from this range are suitable; the most frequently used DFBs work at 1310 nm or at 1550 nm. DFB lasers are cheap, offer relatively narrow spectrum of emitted wavelengths; however, the stability of wavelength is usually worse than in He-Ne lasers. One has to consider the fact that detected number of fringes detected at the observation plane depends on wavelength. Because of this fact, stabilized lasers with a temperature controller can be used. This makes the arrangement more expensive. Since DFB lasers usually work stable in temperature a bit lower than room temperature, one has to wait few minutes until the temperature of a chip is

achieved and the emitted wavelength is stabilized. In addition, since the emitted wavelength is not from the visible range, the feedback about the interference fringes is not available for human eye. It is necessary to use a detection circuit (e.g. a photodiode and an oscilloscope) to observe time changes of an interferogram at an observation point. In general, low fringe contrast indicates that some adjustments are required.

An interferometer with long arms must fulfill the condition of coherence length (simplifying, the path taken of all the interfering waves must differ by less than a coherence length, which differs for a LED, white light and lasers). Otherwise interference is not observed. The best coherence length refers to lasers. For example the coherence length of a single mode He-Ne laser can exceed 100 m, while some LED sources exhibit the coherence length of few centimeters.

Objects absorbing the laser beam's energy require using stronger optical power. For this purpose, one can use Argon ion lasers operating at 510 or 490 or 350 nm, exhibiting the power reaching few Watts [7]. Laser diodes, on the contrary, can offer the variety of available wavelengths from infrared to ultraviolet region, however, usually not exceeding the power of tens mW. Multimode lasers usually have worse coherence length than single mode lasers. CO_2 lasers operating in the infrared region can be useful for measurements over long distances.

Wavelength stability influences the accuracy of results. The change in length of the measuring arm of an interferometer is the multiple of wavelength, as expressed in the formula (21).

$$\Delta l = 0.5 \cdot \lambda \cdot n \tag{21}$$

where λ is wavelength, n is number of counted fringes. He-Ne laser exhibits good wavelength stability, for stabilized lasers is fraction of MHz, non-stabilized lasers are usually one range of order worse. Pay attention to older lasers, the real operation wavelength range can differ from nominal range. The knowledge on wavelength instability is often required to evaluate the accuracy of results dependent on λ. If you do not know the wavelength tolerance, you can calculate it from the formula (22):

$$\Delta\lambda = \frac{\lambda_c^2}{c}\Delta f \tag{22}$$

For example, for a He-Ne laser operating at λ=632.8 nm ±2 MHz (as usually expressed in a catalogue), the equivalent expression is λ=632.8 nm ± 2.7 10^{-6} nm, from which it can be concluded that the wavelength instability is negligible.

$$\Delta\lambda = \frac{\lambda_c^2}{c}\Delta f = \frac{\left(632.8 \cdot 10^{-9}\right)^2}{3 \cdot 10^8} \cdot 2 \cdot 10^6 = 2.7 \cdot 10^{-15} m = 2.7 \cdot 10^{-6} nm \tag{23}$$

A practical remark referring to lasers used in interferometry refer to a safety class of used laser. It is recommended to check the safety class, which should be displayed on a label and informs about the necessary protection, which can for example be the use of special protection glasses. In addition, it is not recommend looking into the laser's aperture and avoiding the eye contact with the back reflections from any surface. The direct beam from even a low-power He-Ne laser (0.5 mW) can cause serious eye damage [7].

3.4. Detection of fringes and evaluation of measurement

Different detection methods can be used based on the properties of the measured signals (high speed or slow signals, periodic or nondeterministic signals, low amplitude signals) as well as on the properties of used laser. In general, detection of fringes allows using different devices, such as photodiodes, photomultipliers, photoconductive detectors, CCD sensors or pyroelectric detectors. Photodiodes as the most popular and universal detectors cover wide range of wavelengths, photoconductive detectors are used in the infrared region. Pyroelectric detectors are sensitive over the infrared region, but in addition, they respond to changes in illumination. However, the most sophisticated detection devices assume a detection unit integrated with the circuits for signal processing, including amplification, Fourier transform of a signal suitable for monitoring the frequency changes of an investigated process, and last but not least, converting the measured signal for its transmission (sampling, quantization, encoding, and many others). One of the cheapest solutions is to use commercially available fringe counters or a photodiode with an operational amplifier and to process the signal on a computer. For some applications (i.e. those assuming slow time variations of fringe distribution with the frequency much lower than 1 Hz), it is sufficient to use a spectral analyzer.

Most of affordable optical fibers as well as the majority of fiber optic components are designed to operate at 1300 or 1550 nm and exhibit huge attenuation in the visible range.

When the optical path length of one arm is changed, the distribution of interference fringes on an observation point varies in time. It is possible to monitor their shift, direction and density. For some applications in low speed signal measurement, a spectral analyzer is sufficient, but for signals requiring fast sampling, huge amplification and low noises, a photodiode with an operational amplifier and an oscilloscope is optimal. Another solution is the use of fringe counters; however, they offer poor feedback compared to specialty purposes photodetectors.

The emergence of new fringes is relatively slow from the perspective of a detector. Number of samples measured by a detector per unit of time must be at least twice of the maximum number of occurring interference fringes per unit of time, as according to the Nyquist theorem [12]. For detection of weak signals (few nanowatts), we use a fast response, low noise photodiode integrated with an operational amplifier. Time variation of light intensity is displayed on an oscilloscope.

The measurements can be done with optical shielding to forbid the reception of the disturbing signals. For this purpose, the photodetector is usually bounded into a box with an aperture (without diffraction). To count fringes, the aperture accepts one fringe at a moment. The

interferometer is calibrated to display one fringe in the observation plane. More fringes in the aperture could cause that a new fringe is unnoticed.

Localization of fringes in Michelson interferometers can be done using Fourier optics. The analysis presented in [13] helps to understand the Michelson fringes. It can be used for testing optical elements such as mirrors, beam splitters, polarizers and collimation of lenses.

Knowing the number of fringes detected on an observation plane, it is possible to calculate the change in length of the measuring arm from the formula (21). Changes to a measured quantity is proportional to variation in measuring arm length, it is assumed the relation between measured quantity and measuring arm is known. Initial values of the measured quantity must be known since Michelson interferometer is not able to measure absolute values (such as temperature, length) but their differential from the initial values (such as temperature changes, elongation etc.). However, the modified circuits can provide the information about the absolute values, there is a paper about absolute distance meter [14].

A separate problem is the accuracy of obtained results. Repeatability of results could roughly confirm accuracy. In addition, there are few techniques to verify it in theory. The precision of Michelson setup reaches the order of half-wavelength of the He-Ne laser. One fringe corresponds to the change in path length equal to 0.5x632.8 nm, assuming the He-Ne laser. The greater precision can be achieved by using a shorter wavelength. However, much shorter wavelengths are not compatible with most of affordable components. Few methods exist to estimate measurement errors from gathered data and determine resultant accuracy of the calculated results. The most popular one is the exact difference method [15]. The method is suitable for estimation of overall accuracy of multi-tasking measurement and is widely used in physics and engineering, for its statistical accuracy and simplicity. The method can evaluate the optical part of experiment, i.e. Michelson interferometer, but it also enables to combine its accuracy with accuracy of other accompanying measurements, necessary to calculate the result. The general idea is expressed by the formula (24).

$$\Delta a = \sum_{i=1}^{n} \left| \frac{\partial a}{\partial q_i} \right| \cdot \Delta q_i \tag{24}$$

Where a is measured quantity (i.e. parameter, coefficient) being the function of particular quantities directly measured on an investigated object q_i and Δ is inaccuracy). For example, q in formula (24) can be wavelength accuracy or number of read fringes. It can be reading the initial value of measured quantity, the precision of initial value taken from a catalog or accuracy of any accompanying measurement, e.g. time, temperature etc. (The result can be the function of arm's length changes as well as the function of many other processes, not measured by the interferometer). Exact difference method allows combining the contribution of all the measured quantities to overall accuracy.

In practice, results should have the desired form, i.e. they should be stored in a file for further processing on a computer, such as Fourier transform, which is suitable for measuring frequency of vibrations etc. The processing circuit has been proposed in [16].

http://dx.doi.org/10.5772/57149

4. Exemplary experiments

The most investigated application of a Michelson interferometer is a fiber optic sensor [17]. It can measure displacement [18], length changes, amplitude of vibrations (e.g.) the amplitude of seismic waves [19], resonant frequency of vibration, changes in temperature [20], strain (perimeters) [21], and many others. We present the applications to a measurement of thermal expansion coefficient by using a free-space Michelson setup and the application to a measurement of amplitude of vibration of a loudspeaker and its frequency by using a fiber optic Michelson interferometer. Both examples offer a good illustration of the principle of operation of Michelson interferometer and help to understand the procedure of how to build an interferometer.

4.1. Measurements of linear expansion and calculation of thermal expansion coefficient using free space Michelson interferometer

There are few approaches to how to obtain the thermal expansion coefficient; however, high accuracy can be achieved by using noncontact optical methods. A generally accepted view is that if solid is heated, its volume increases. General volumetric thermal expansion coefficient is given as:

$$\alpha_v = \frac{1}{V} \cdot \frac{\partial V}{\partial T} \tag{25}$$

where V is volume entering the process at the condition of constant pressure and T is time. In solids, the pressure does not appreciably affect the size of an object. To an approximation with regard to measurement, the change in length of an object (which is linear dimension as opposed to volumetric dimension) due to thermal expansion is related to a temperature change by a linear expansion coefficient, which is defined as linear expansion due to a change in temperature with respect to initial length of an object, as shown in (26) and is expressed in K^{-1} [22]:

$$\alpha = \frac{\Delta l_t}{l_0 \cdot |T_2 - T_1|} \tag{26}$$

where α is thermal expansion coefficient, Δl_t – linear expansion; l_0 – initial length; T_1 is initial temperature and T_2 is final temperature.

Linear expansion denoted as Δl_t depends on initial length l_0 of an object and change in temperature. The thermal expansion coefficient can be obtained from data for either heating or cooling process. It does not depend on the shape of the object, temperature range or speed (i.e. how intense is the heating process). Linear expansion Δl_t of a solid measured by an interferometer is shown in (27) and is expressed in meters [4]:

$$\Delta l_t = 0.5 \cdot \lambda \cdot n \tag{27}$$

where n is number of interference fringes passed through an observation point of an interferogram, obtained with respect to optical path difference, and λ is wavelength of the laser as a source of coherent optical radiation. The measurement of temperature and the measurement of linear expansion must be done together. To determine a thermal expansion coefficient, the initial length of an investigated object must be well known.

Substituting (27) to (26) and knowing the initial and final temperature, it can be obtained:

$$\alpha = \frac{0.5 \cdot \lambda \cdot n}{l_0 \cdot |T_2 - T_1|} \tag{28}$$

The thermal expansion coefficient is constant for a given material. Thermal expansion coefficient can be determined for small linear expansion (i.e. achieved for a small change in temperature). Since temperature affects distribution of interference fringes, the experiment can be carried out in room temperature that facilitates temperature controllability. The block scheme of an experimental setup using a free space Michelson interferometer for measurement of thermal expansion coefficient of a copper rod is presented in Figure 6, and the practical arrangement is shown in Figure 7.

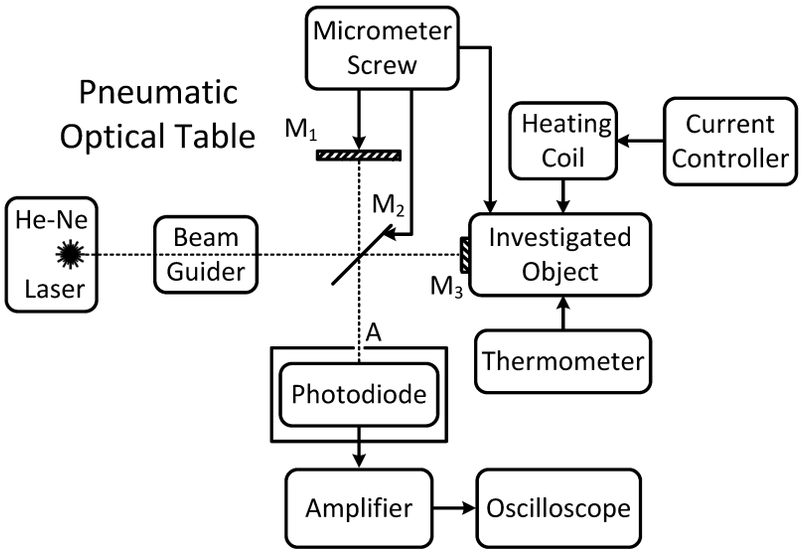

Figure 6. Schematic diagram of a free space Michelson interferometer for the measurement of thermal expansion coefficient for copper. M_2 – 50% mirror (beam splitter), M_1, M_3 – dielectric mirrors.

http://dx.doi.org/10.5772/57149

Figure 7. Schematic diagram of a free space Michelson interferometer for the measurement of thermal expansion coefficient for copper. 1, 2 – dielectric mirrors, 2 – beam splitter, 4 – observation plane (left), and detailed view on the investigated object (1) placed in a holder (2) with a micrometer screw (3), plastic isolation (4), heating coil, and a mirror in a mount (6) (right).

Optical path difference corresponding to one fringe is equal to value of half-wavelength. To obtain the value of linear expansion of a material, the value of half-wavelength is multiplied by the number of interference fringes. Data are gathered for monotonic increase in temperature. In general, temperature changes do not have to be monotonic because the key feature is to know an initial and final temperature, however, to facilitate fringe counting it is better to measure them at the condition of monotonic change in temperature. If the temperature change is not monotonic and both heating and cooling occur between an initial and final temperature, some fringes are measured several times and as a result the measured expansion is larger than it is in reality. Heating can be done by a coil, cooling is natural and is not accelerated by any cooling device. The measurement should be repeated many times and the measured values should be averaged in order to ensure the credibility of measurement.

The investigated object can be a metal rod with well-known initial length. A dielectric mirror should be placed on the tip of the rod and terminates the interferometer's arm. It is a high reflectance dielectric mirror created by the deposition of a thin layer of a dielectric material on a glass substrate. Eventual unexpected variation in room temperature could influence the path length and the distribution of fringes. For this reason, e.g. a gas burner cannot be used for heating.

We determine the thermal expansion coefficient for copper from the measured number of fringes, the initial rod's length and the temperature change. The number of light intensity maxima (i.e. the number of light fringes) multiplied by the value of half-wavelength is equal to the resultant expansion of the investigated copper rod. The result is averaged. For a well-known value of thermal expansion coefficient, the experimental setup can also work as a very accurate sensor of temperature changes that could for example be used in monitoring temperature stability in harsh environment. A similar application has been published [20]. Sample measured interferograms are shown in Figure 8.

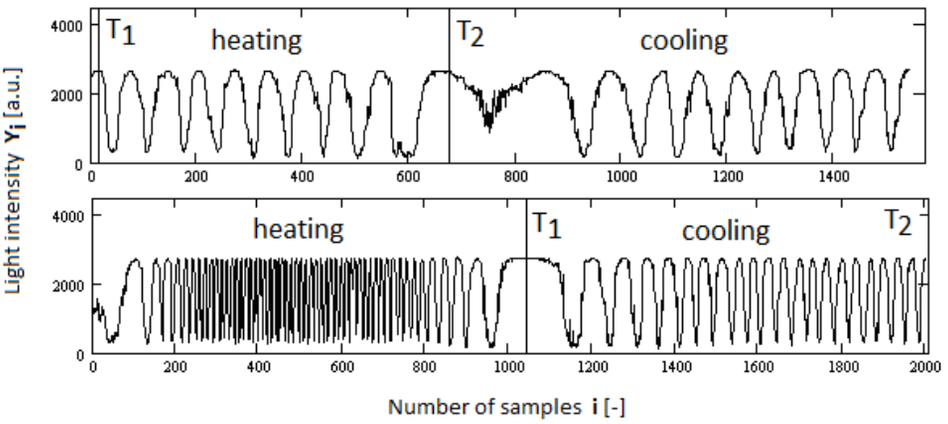

Figure 8. Sample data on measured light intensity over number of samples. T_1 is initial temperature and T_2 is final temperature of the measurement.

Table 1 shows measured data and the calculated thermal expansion coefficient. In Table 1, l_0 is initial length of the copper rod, T_1 is initial temperature, T_2 is final temperature, n is number of interference fringes, λ is He-Ne wavelength, Δl_t is linear expansion, and α is thermal expansion coefficient calculated using (24).

l_0	T_1	T_2	$\lvert T_2-T_1 \rvert$	n	λ	Δl_t	α
(m) x10^{-3}	(K)	(K)	(K)	(-)	(m) x 10^{-9}	(m) x 10^{-6}	(K^{-1}) x 10^{-6}
82	296.7	317.5	20.8	105	632.8	33.222	19.47819
82	317.7	307.2	10.5	45	632.8	14.238	16.53659
82	312.8	301.3	11.5	49	632.8	15.504	16.44072
82	301.1	296.8	4.3	18	632.8	5.695	16.15201
82	296.7	302.7	6	27	632.8	8.543	17.36341
82	303.9	296.9	7	31	632.8	9.808	17.08780
82	296.8	301.0	4.2	20	632.8	6.328	18.37398
82	305.3	297.2	8.1	38	632.8	12.023	18.10178
82	323.3	303.3	20	92	632.8	29.109	17.74927
82	303.3	309.8	6.5	29	632.8	9.176	17.21501
82	305.2	303.0	2.2	10	632.8	3.164	17.53880
82	296.9	300.9	4	18	632.8	5.695	17.36341
82	297.3	315.6	18.3	80	632.8	25.312	16.86792
Mean							**17.40530**

Table 1. Calculation of a thermal expansion coefficient for copper.

The averaged value of thermal expansion coefficient, 17.4 $K^{-1}x10^{-6}$, corresponds well to the value 16.9 $K^{-1}x10^{-6}$ that can be found in [23].

http://dx.doi.org/10.5772/57149

4.2. Measurement of membrane vibration frequency using fiber optic Michelson interferometer

A schematic diagram of the experimental setup using a fiber optic Michelson interferometer for measurement of membrane vibration frequency is presented in Figure 9.

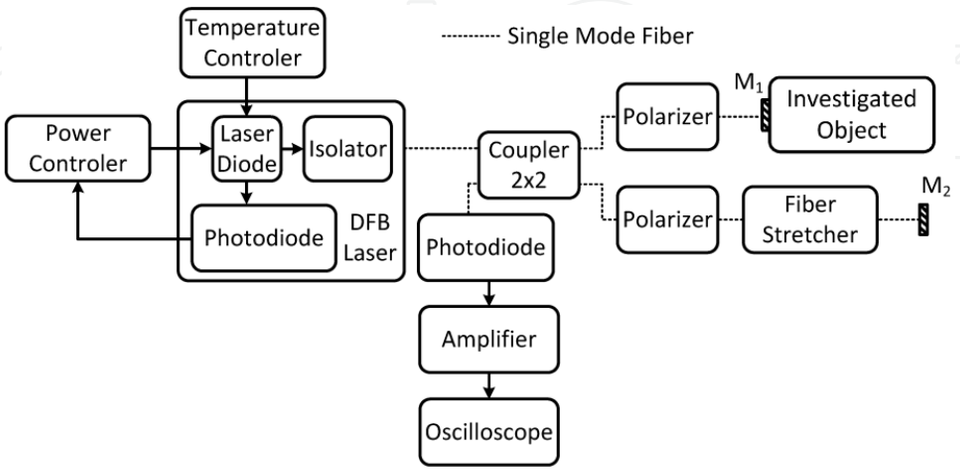

Figure 9. Schematic diagram of a fiber optic Michelson interferometer for the measurement of membrane vibration frequency. M_1, M_2 – pigtailed dielectric fiber mirrors.

The reference DFB laser beam is guided to the observation plane, going twice through the coupler. The measuring beam is guided to the investigated object, which is a loudspeaker mounted on a fiber mirror. As a result of the superposition of the two beams, interference fringes are observed. The interference fringes pass to a photo detector with an amplifier, and the maxima of signal intensity are displayed on an oscilloscope. Finally, data are exporter to PC.

The experimental setup should suppress ambient vibrations; otherwise the interference pattern is not stable. The experimental setup is placed on a hydro-pneumatic laboratory table and mounted by using special holders. Practical arrangement of the experimental setup is shown in Figure 10. The DFB laser operate at 1300 nm. Its temperature is monitored and controlled in order to provide a stable wavelength in time and narrow emitted bandwidth. Pigtailed mirrors, fiber couplers, polarizers are commercially available. The oscilloscope provides Fourier transform of the measured signal in order to measure the known frequency of vibrations of a loudspeaker.

The model of a high-speed and low amplitude physical quantity can be represented by the signal originated by the loudspeaker's membrane. The measurements were performed on a small 0.5W 8Ω, loudspeaker with the operation bandwidth 4 Hz – 1.8 kHz. The excitation signal is a sinus wave with constant amplitude. The excitation signal must not contain a constant voltage component, which causes the short circuit and can damage the loudspeaker. (To avoid this, a loudspeaker should be supplied through a capacitor). If a waveform generator is equipped with output impedance greater than tens of ohms, the loudspeaker should be connected to the generator with a resistor in series. However, too large resistance causes absorption of vibrations.

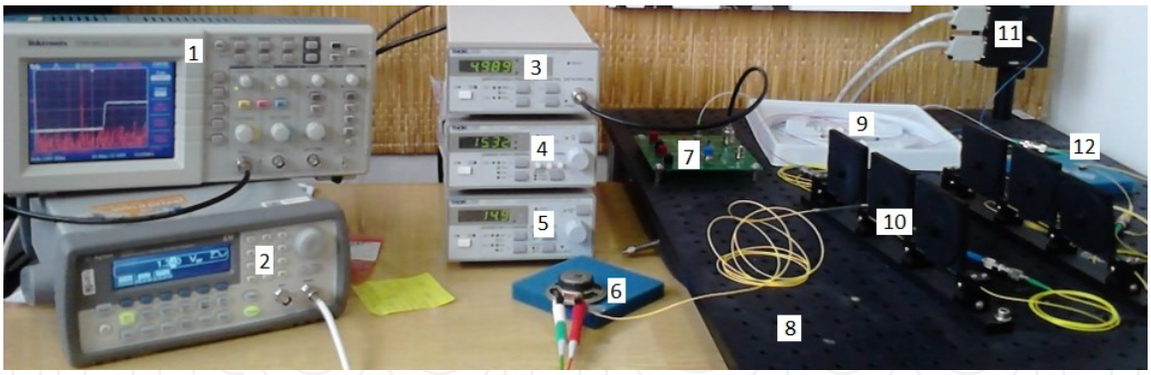

Figure 10. Practical arrangement of a fiber optic Michelson interferometer for the measurement of membrane vibration frequency. 1 – oscilloscope, 2 – waveform generator, 3 – electric amplifier, 4 – temperature controller, 5 – laser power controller, 6 – investigated object – a loudspeaker, 7 – photodiode, 8 – optical table, 9 – fiber coupler, 10 – polarizer, 11 – DFB laser in a special holder, 12 – pigtailed fiber mirror.

A fiber dielectric mirror mounted on the loudspeaker oscillates with its membrane. The information on its displacement is contained in the interference fringes. For rough measurement of vibration's frequency (but not precise determination of amplitude of vibrations), it is sufficient to place a loudspeaker close to the fiber mirror.

The change in light intensity on the detector's surface is caused by the vibration of the investigated membrane. The amount of fringes passing through the slit in front of an interference pattern corresponds to certain displacement of the membrane. Sample measured data is displayed in Figure 11.

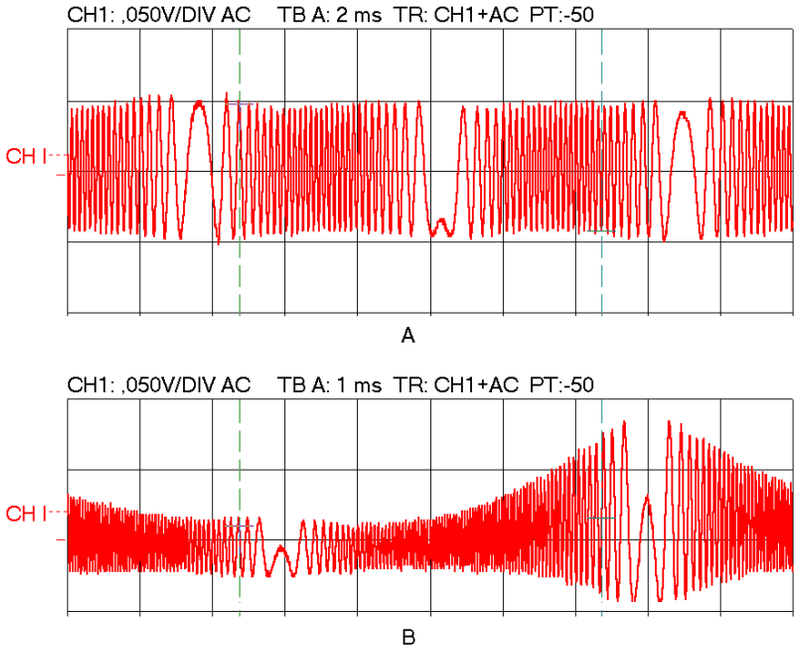

Figure 11. Sample data describing vibrations of a membrane. Frequency of oscillations: 75 Hz, number of maxima per period: 59 (A), and 99 Hz, number of light intensity maxima per period being 164 (B).

The broadened pitch between two light intensity maxima indicates the change to the direction of movement of the membrane. The amplitude of membrane's vibrations can be calculated by using (21). The circuit can measure the frequency of loudspeaker's sound (i.e. the frequency of membrane vibrations) by setting the Fourier transform on an oscilloscope. If the frequency is known, it can be a tool to verify that the setup works correctly. Then the frequency at a waveform generator connected to a loudspeaker should correspond well to the frequency measured and displayed on an oscilloscope. In addition, maximum vibration is measured for the resonant frequency.

5. Conclusions

The main advantage of the laser interferometry method is its precision, noncontact procedure and the application to objects specific for the small variation of signals measured on them. The experimental results confirmed the high accuracy of this optical method in this specific application area.

The measurements require performing many supplementary measurements. Every measurement is the source of inaccuracy. One has to consider potential inaccuracy sourcing from thermometers, length meters, lasers, as well as find the right solution for the detection and processing of fringes. Michelson interferometer requires mechanical stability especially in a free space arrangement to reduce spurious signals, strongly affecting the final result.

Considering the coherence length, the interferometer can be distributed to allow for measurement on far objects. In addition, the interferometer can be miniaturized or built as a fiber optic based sensor.

Acknowledgements

This work was supported by the Ministry of Interior of the Czech Republic grant under project VG20102015053, "Guardsense" and by the by the CTU grant under project SGS13/201/OHK3/3T/13.

Author details

Michal Lucki*, Leos Bohac and Richard Zeleny

*Address all correspondence to: lucki@fel.cvut.cz

Department of Telecommunications Engineering, Faculty of Electrical Engineering, Czech Technical University in Prague, Prague, Czech Republic

References

[1] Malak M., Marty. F., Nouira H., Salgado J. A., Bourouina T. All-silicon interferometric optical probe for noncontact Dimensional measurements in confined Environments. Proceedings of the IEEE 25th International Conference on Micro Electro Mechanical Systems; 2012 628-631. http://ieeexplore.ieee.org/xpl/articleDetails.jsp?tp=&arnumber=6170266&queryText%3DAll-silicon+interferometric+optical+probe+for+noncontact+Dimensional+measurements+in+confined+Environments (accessed 4 September 2013).

[2] Luhs W. Experiment 10 Michelson interferometer. Eschbach: Laserzentrum FH Münster University of Appl. Sciences; 1995 revised 2003. http://repairfaq.ece.drexel.edu/sam/MEOS/EXP10.pdf (accessed 4 September 2013).

[3] Mokryy O., Koshovyy V., Romanyshyn I., Sharamaga R. Stabilized detection scheme of surface acoustic waves by Michelson interferometer. Optica Applicata 2010; 40(2) 449-458. http://www.if.pwr.wroc.pl/~optappl/pdf/2010/no2/optappl_4002p449.pdf (accessed 4 September 2013).

[4] Scholl R., Liby B. W. Using a Michelson Interferometer to Measure Coefficient of Thermal Expansion of Copper. The Physics Teacher 2009; 47(5) 316-318. http://physlab.lums.edu.pk/images/2/2c/Scholl_liby.pdf (accessed 4 September 2013).

[5] Tol J., A Mach-Zehnder-interferometer-based low-loss combiner. Photonics Technology Letters 2001; 13(11) 1197-1199. http://ieeexplore.ieee.org/xpl/articleDetails.jsp?tp=&arnumber=959362&queryText%3DTol+J.%2C+Huig+G.%2C+Yong+L.+A+Mach-Zehnder-interferometer-based+low-loss+combine.+Photonics+Technology+Letters (accessed 4 September 2013).

[6] Fang X. A variable-loop Sagnac interferometer for distributed impact sensing. Lightwave Technology 1996; 14(10) 2250-2254. http://ieeexplore.ieee.org/xpl/articleDetails.jsp?tp=&arnumber=541215&queryText%3DA+variable-loop+Sagnac+interferometer+for+distributed+impact+sensing (accessed 4 September 2013).

[7] Hariharan P. Basics of interferometry. Sydney: School of Physics, University of Sydney, Elsevier; 2007

[8] Zagar B. A laser-interferometer measuring displacement with nanometer resolution. IEEE Transactions on Instrumentation and Measurement 1994; 43(2) 332-336. http://ieeexplore.ieee.org/xpl/articleDetails.jsp?tp=&arnumber=293440&queryText%3DA+laser-interferometer+measuring+displacement+with+nanometer+resolution (accessed 4 September 2013).

[9] Iyer S., Coen S., Vanholsbeeck F. All-fiber optical coherence tomography system incorporating a dual fiber stretcher dispersion compensator. Proc. SPIE 7004, 19th International Conference on Optical Fibre Sensors; 2008, 700434-1–700434-4. http://

proceedings.spiedigitallibrary.org/proceeding.aspx?articleid=786962 (accessed 5 September 2013).

[10] Winter A., Schlarb H., Schmidt B., Ilday F.O., Jung-Won Kim Chen J., Grawert F.J., Kartner F.X. Stabilized Optical Fiber Links for the XFEL. Proceedings of the Particle Accelerator Conference; 2005 2589-2591. http://ieeexplore.ieee.org/xpl/articleDetails.jsp?arnumber=1591192 (accessed 4 September 2013).

[11] Kersey A. D., Marrone M. J., Dandridge A., Tveten, A. B. Optimization and Stabilization of Visibility in Interferometric Fiber-optic Sensors Using Input-Polarization Control. Journal of Lightwave Technology 1988; 6 (10) 1599-1609.

[12] Diniz P., Da Silva E., Netto S. Digital Signal Processing: System Analysis and Design. Cambridge: Cambridge University Press; 2002. http://assets.cambridge.org/97805217/81756/copyright/9780521781756_copyright.pdf (accessed 4 September 2013).

[13] Narayanamurthy C. S. Analysis of the localization of Michelson interferometer fringes using Fourier optics and temporal coherence Eur. J. Phys. 2009; 30 147-155. http://iopscience.iop.org/0143-0807/30/1/015/pdf/ejp9_1_015.pdf (accessed 4 September 2013).

[14] Alzahrani K., Burton D., Lilley F., Gdeisat M., Bezombes F. Automatic Absolute Distance Measurement with One Micrometer Uncertainty Using a Michelson Interferometer. Proceedings of the World Congress on Engineering; 2011, Vol 2. http://core.kmi.open.ac.uk/display/1019144 (accessed 4 September 2013).

[15] Boyce W., Di Prima R. Elementary Differential Equations. New York: John Wiley & Sons, Inc.; 1986.

[16] Cheng K., Shang X., Cheng X. The Digitization of Michelson Interferometer. Proc. of 2011 International Conference on Electronics and Optoelectronics; 2011 V3142-V3145.

[17] Byeong H. L., Young H. K., Kwan S. P., Joo B. E., Myoung J. K., Byung S. R., Hae Y. Ch. Interferometric Fiber Optic Sensors. Sensors 2012; 12 2467-2486. http://www.mdpi.com/1424-8220/12/3/2467 (accessed 4 September 2013).

[18] Yung-Cheng W., Lih-Horng S., Chung-Ping Ch. The Comparison of Environmental Effects on Michelson and Fabry-Perot Interferometers Utilized for the Displacement Measurement. Sensors 2010; 10 2577-2586. http://www.mdpi.com/1424-8220/10/4/2577 (accessed 4 September 2013).

[19] Acernesea F., De Rosab R., Garufi F., Romano R., Barone F. A Michelson interferometer for seismic wave measurement: theoretical analysis and system performances. Proc. SPIE 6366 Remote Sensing for Environmental Monitoring, GIS Applications, and Geology VI; 2006. http://spie.org/x648.html?product_id=687907 (accessed 4 September 2013).

[20] Li X., Lin S., Liang J., Zhang Y., Ueda O. Fiber-Optic Temperature Sensor Based on Difference of Thermal Expansion Coefficient Between Fused Silica and Metallic Ma-

terials. IEEE Photonics Journal 2012; 4(1) 155-162. http://ieeexplore.ieee.org/xpl/articleDetails.jsp?tp=&arnumber=6112705&queryText%3DFiber-Optic+Temperature+Sensor+Based+on+Difference+of+Thermal+Expansion+Coefficient+Between+Fused+Silica+and+Metallic+Materials

[21] Kezmah M., Donlagic D., Lenardic B. Low Cost Security Perimeter Based on a Michelson Interferometer. Proc of IEEE Sensors; 2008 1139-1142. http://ieeexplore.ieee.org/xpl/articleDetails.jsp?tp=&arnumber=4716642&queryText%3DLow+cost+security+perimeter+based+on+a+Michelson+interferometer (accessed 4 September 2013) (accessed 4 September 2013).

[22] Cverna F., editor. ASM International Materials Properties Database Committee. Thermal Properties of Metals. ASM Materials Data Series; 2002. http://www.asminternational.org/content/ASM/StoreFiles/ACFAAB7.pdf (accessed 4 September 2013) (accessed 4 September 2013).

[23] Chapter12. In: Lide D. CRC Handbook of Chemistry and Physics, Boca Raton: CRC Press; 2003. http://www.hbcpnetbase.com/ (accessed 4 September 2013).